Transactions C: Chemistry and Chemical Engineering
Vol. 17, No. 2, pp. 158–167

SCIENTIA IRANICA

Modeling of Methane and Propane Hydrate Formation Kinetics Based on Chemical Affinity

F. Varaminian[1,*] and A.A. Izadpanah[2]

Abstract. *In this study, experimental data on the kinetics of methane and propane hydrate formation at constant volume were collected. The experiments were carried out in a batch reactor under different temperatures and pressures. The chemical affinity was used for modeling of the hydrate formation rate in a constant volume process. In this method, the system was considered as a classical thermodynamic or macroscopic view. The results show that this method can predict constant volume experimental data well for both crystals I and II hydrate former.*

Keywords: *Chemical affinity; Methane; Propane; Formation kinetics; Gas hydrates.*

INTRODUCTION

Gas hydrates are crystalline solids. They are composed of polyhedra of hydrogen bonded water molecules. The crystalline structure forms cages that contain at most one small guest molecule. At low temperatures, close to the freezing point of water, and under high pressure, these guest molecules, which are a large variety of gases or volatile liquids, can form gas hydrates when they came into contact with water, under certain conditions.

Many different thermodynamic models have been suggested for predicting hydrates [1,2], but more studies must be undertaken regarding their formation and decomposition rate. There are many different views about the hydrate formation process. A semi-empirical model was proposed for the gas consumption rate [3,4]. Later, an intrinsic kinetics model for hydrate growth, with only one adjustable parameter, was formulated [5]. Hydrate formation is also proposed by nucleation and growth processes. It is very difficult to distinguish between nucleation and growth rate, since both processes occur simultaneously. Much research work on different models is based on mass and heat transfer that control mechanisms [6,7], but because of the complexity and stochastic nature of the process, a model is needed that uses the initial and final condition of the process to predict the formation rate.

In this work, a chemical affinity was used for modeling the hydrate formation rate under a constant volume process. Moreover, an experimental setup was set up to collect hydrate formation data.

MATERIALS AND PROCEDURES

The experiments were undertaken in a system that consists of a reactor, a shell for heat transfer and a data acquisition system. The apparatus is shown in Figure 1.

The hydrate formation reactor was made using a 3/4 inch Schedule No. 80, stainless steel 316 pipe. At the two ends of these pipes, a pressure transmitter and a thermometer were installed. The volume of the reactor was 120 cc. In order to heat and cool the system, the hydrate formation reactor was converted to a shell and tube by a polyethylene shell. The cell pressure was measured using a Druck PTX1400 pressure transmitter (0-10 MPa) with an accuracy of about ±0.25% of the scale (i.e. 25 kPa). The temperature was measured using PT100 thermometers with an accuracy of ±0.1 K. The signals of pressure and temperature were acquired by a data acquisition system driven by a personal computer. The cell pressure and temperature data from the acquisition system were saved at preset sampling intervals on a computer hard disk. The temperature of the reactor was controlled by the flow of an ethanol-water solution, using an external circulating temperature bath through

1. *Department of Chemical Engineering, Engineering Faculty, Semnan University, Semnan, Iran.*
2. *Department of Chemical Engineering, Engineering Faculty, Persian Gulf University, Bushehr, P.O. Box 7516913798, Iran.*
*. *Corresponding author. E-mail: fvaraminian@semnan.ac.ir*

Received 5 June 2009; accepted 10 April 2010

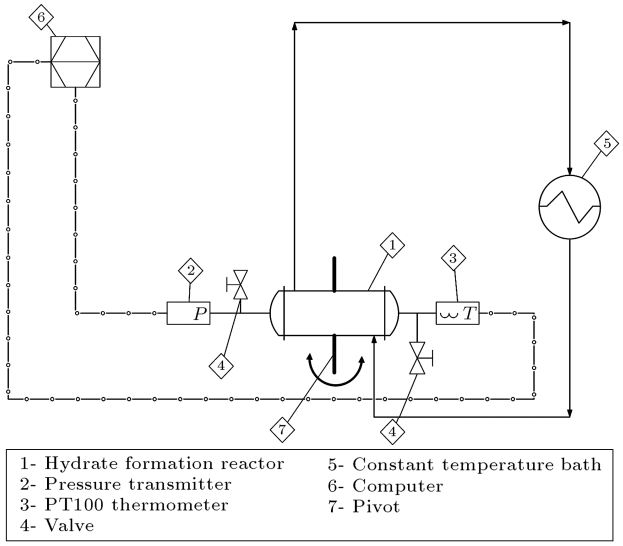

Figure 1. Experimental setup, hydrate formation apparatus.

the shell. A Lauda RE 210 temperature bath was used to control the temperature of the cooling fluid.

The reactor was mounted on a pivot and the mixing was obtained by rocking the cell. Methane (a hydrate former, crystal I) with nominal purity (99.999%) and propane with nominal purity (99.95%) supplied by air product and distilled water were used. First, the hydrate formation reactor was evacuated. 30 cc of mercury and 40 cc of distilled water were charged to the reactor. The reactor was then pressurized to about 0.05 MPa below the equilibrium pressure for the hydrate formation at the specified experimental temperature. The constant temperature bath was turned on and the reactor was allowed to reach the constant experimental temperature. When the solution attained thermal equilibrium, the reactor was pressurized to the experimental pressure by supplying gas from the cylinder; mixing was started and data collection began.

MODELING

Chemical Affinity

Chemical affinity, A, is defined as a generalized driving force for chemical reactions as [8]:

$$A = -\sum_i \nu_i \mu_i, \tag{1}$$

where μ_i is the chemical potential of component i. According to the definition at equilibrium condition the affinity is equal to zero and in any state that the reaction proceeds spontaneously, the affinity is positive.

Classically, the chemical potential μ_i of component i in any arbitrary state can be related to its chemical potential, μ_i^0, in some standard state by an equation of the form:

$$\nu_i \mu_i = \nu_i \mu_i^0 + RT \ln(a_i)^{\nu_i}, \tag{2}$$

where R is the gas constant and a_i is the activity of component i.

Equation 2 can be expressed in terms of affinity by substituting from Equation 1 to yield:

$$A = A^0 - RT \sum_i \ln(a_i)^{\nu_i}, \tag{3}$$

where A^0 is the affinity of the reacting system, if the components are in their standard state and A is only a function of temperature. If an activity ratio, Q, is defined as:

$$Q = \prod_i (a_i)^{\nu_i}, \tag{4}$$

then, Equation 4 can be rewritten as:

$$A = A^0 - RT \ln(Q), \tag{5}$$

at reaction initiation $Q = 0$, so that $A = \infty$, while at equilibrium $A = 0$, $A^0 = RT \ln(K)$, where K is the thermodynamic equilibrium constant. Substituting for A^0 in Equation 5 yields:

$$A = -RT \ln(\zeta_Q), \tag{6}$$

where:

$$\zeta_Q = \left(\frac{Q}{K}\right).$$

By definition the value of ζ_Q is limited to the range $0 \leq \zeta_Q \leq 1$, and its standard state value, ζ_Q^0, is equal to $\frac{1}{K}$. Hence, ζ_Q is a dimensionless measure of the extent of reaction from $A = \infty$ to $A = 0$.

Accordingly, for any chemical reaction proceeding spontaneously in a closed system of fixed volume V and constant temperature T, the affinity decays towards zero so that:

$$\dot{A}_{Ty} < 0, \tag{7}$$

where:

$$\dot{A}_{T,V} = \left(\frac{\partial A}{\partial t}\right)_{T,V},$$

is the affinity decay rate.

The calculated values of $\dot{A}_{T,V}$ were correlated with various functions of elapsed time, t_i, by a regression analysis to determine the best data fit. However, as soon as the reciprocal-time relationship was examined, it was apparent that $\dot{A}_{T,V}$ was inversely proportional to the elapsed time [9]:

$$\dot{A}_{T,V} \propto \frac{1}{t} + I. \tag{8}$$

Because $\dot{A}_{T,V} = 0$ at the equilibrium (or end of reaction), the intercept (I) must depend on the time

of achieving the equilibrium (t_K), and it can rearrange Equation 8 to:

$$\dot{A}_{T,V} = A_r \left[\frac{1}{t} - \frac{1}{t_K}\right], \tag{9}$$

where A_r is a constant of proportionality and denotes the affinity rate constant.

In order to directly correlate the calculated values of the chemical affinity with the measured values of elapsed time, Equation 9 must be integrated, which yields:

$$A_i = A_r \ln\lfloor \zeta_{t_i} . \exp(1 - \zeta_{t_i})\rfloor, \tag{10}$$

where:

$$\zeta_{t_i} = \left(\frac{t_i}{t_K}\right),$$

is similar to ζ_Q, and the extent of reaction ζ_{t_i} is limited to the range $0 \leq \zeta_{t_i} \leq 1$. However, the value of ζ_{t_i} must be known to correlate empirical data by Equation 11 so as to determine the value of t_K, but ζ_{t_i} itself depends on t_K. This obstacle was overcome by generating values of t_K by an iterative subroutine [10].

Hydrate Formation Modeling

As shown in Figure 2, the experimental conditions for hydrate formation must be far away from the 3-phase equilibrium curve (like point A). In constant volume - constant temperature experiments, after the formation of hydrate crystals, pressure decreases gradually because of gas consumption, and the final pressure must be equal to P_{eq} (point B). At this point, hydrate formation stops and the system reaches equilibrium.

In this research, the main assumption is that there is similarity between hydrate formation and chemical reactions under constant T and V conditions. Both processes progress until they reach equilibrium conditions. Then, we supposed that hydrate formation was a chemical reaction similar to the following [11]:

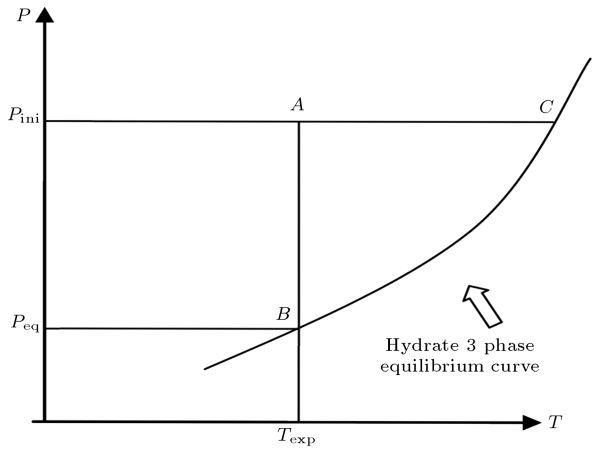

Figure 2. Hydrate formation condition at constant temperature.

$$\sum_{i=1}^{NH} \left(\frac{n_i}{N_{\text{cav}}}\right) g_i + n_w \text{H}_2\text{O} \rightarrow \left[\sum_{i=1}^{NH} \left(\frac{n_i}{N_{\text{cav}}}\right) g_i . n_w \text{H}_2\text{O}\right], \tag{11}$$

where $\frac{n_i}{N_{\text{cav}}}$ and n_w are stoichiometric coefficients of reaction for hydrate formation, gas and water, respectively.

For calculating affinity under different conditions, we must measure the extent of the reaction with time using the pressure of gas at each elapsed time. As shown in Figure 2, the amount of total gas consumed during hydrate formation is equal to $(n_A - n_B)$ and the extent of reaction can be obtained from:

$$\zeta_Q = \frac{n_A - n}{n_A - n_B}. \tag{12}$$

To calculate the number of moles of gas using measured pressure under system conditions, we can use an equation of state to calculate the compressibility of the gas phase and then calculate the number of gas moles as follows:

$$n = \frac{PV}{ZRT}. \tag{13}$$

Now, Equation 12 can be rewritten as:

$$\zeta_{Q_i} = \frac{n_A - n}{n_A - n_B} = \frac{(P_A/Z_A) - (P_i/Z)}{(P_A/Z_A) - (P_B/Z_B)}, \tag{14}$$

and we obtain affinity for each time by the following formula:

$$A_i = -RT \ln(\zeta_{Q_i}). \tag{15}$$

By plotting A_i versus $\ln\lfloor \zeta_{t_i} . \exp(1-\zeta_{t_i})\rfloor$, we can obtain A_r, t_K.

RESULTS AND DISCUSSION

The results for methane at different temperatures and at initial experimental pressure are shown in Figures 3 to 7 for methane and Figures 8 to 10 for propane (because of simplicity, the letter q was shown for ζ_{t_i} in these figures). The compressibility of the gas mixture was calculated from a usual equation of state.

As seen, there is a linear relation between data. The experiments were done for methane at temperatures 274, 276, 278, 280 and 282 K, and for propane at temperatures 274, 275 and 276 K with different

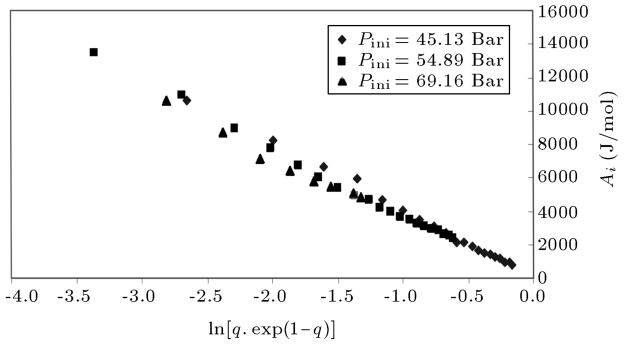

Figure 3. Affinity versus $\ln\lfloor\zeta_{t_i}.\exp(1-\zeta_{t_i})\rfloor$ for methane at 274 K and different initial pressures.

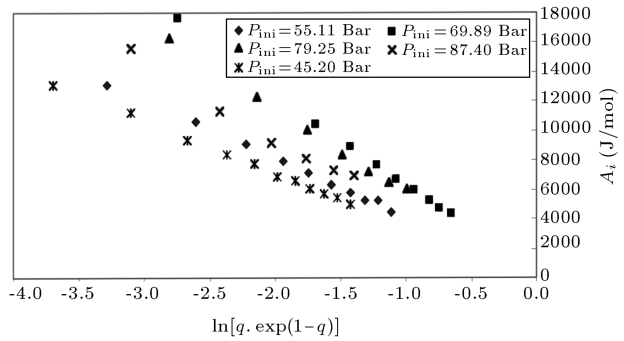

Figure 4. Affinity versus $\ln\lfloor\zeta_{t_i}.\exp(1-\zeta_{t_i})\rfloor$ for methane at 276 K and different initial pressures.

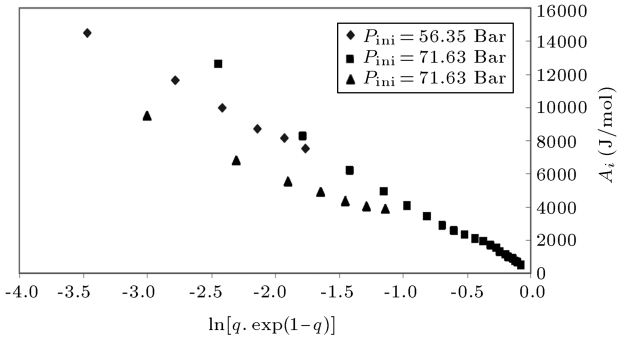

Figure 5. Affinity versus $\ln\lfloor\zeta_{t_i}.\exp(1-\zeta_{t_i})\rfloor$ for methane at 278 K and different initial pressures.

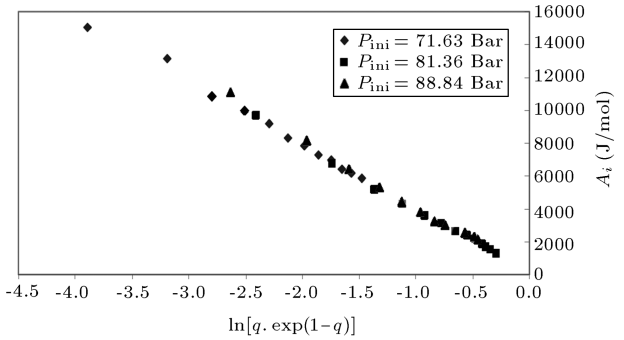

Figure 6. Affinity versus $\ln\lfloor\zeta_{t_i}.\exp(1-\zeta_{t_i})\rfloor$ for methane at 280 K and different initial pressures.

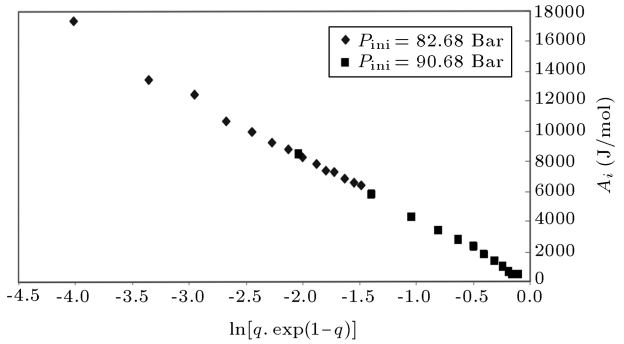

Figure 7. Affinity versus $\ln\lfloor\zeta_{t_i}.\exp(1-\zeta_{t_i})\rfloor$ for methane at 282 K and different initial pressures.

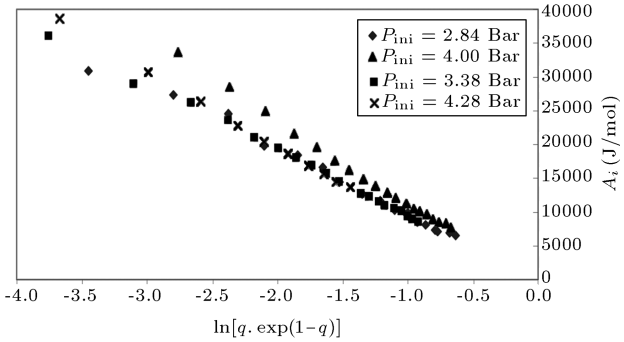

Figure 8. Affinity versus $\ln\lfloor\zeta_{t_i}.\exp(1-\zeta_{t_i})\rfloor$ for propane at 274 K and different initial pressures.

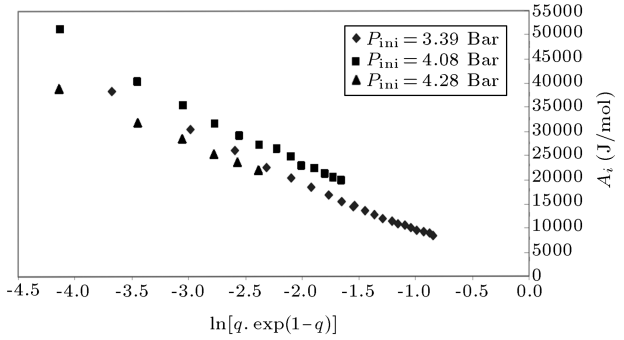

Figure 9. Affinity versus $\ln\lfloor\zeta_{t_i}.\exp(1-\zeta_{t_i})\rfloor$ for propane at 275 K and different initial pressures.

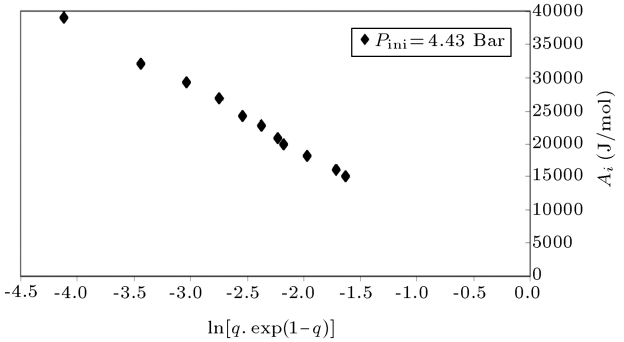

Figure 10. Affinity versus $\ln\lfloor\zeta_{t_i}.\exp(1-\zeta_{t_i})\rfloor$ for propane at 276 K and initial pressure.

initial pressures. The calculated A_r and t_K are given in Table 1 for methane, and in Table 2 for propane.

Variation of reactor pressures with time was calculated using averaged A_r and t_K for each temperature from the results in Tables 1 and 2 for the experiments. In these experiments, the variation of pressures in the hydrate formation reactor with time was measured and shown in Figures 11 (a to q) for methane and Figures 12 (a to h) for propane.

From Figures 11 and 12, we understand that there is good agreement between calculated results and experimental data at low pressure near the 3-phase equilibrium curve in most of the experiments. However, for high pressure experiments, such agreements exist at the beginning of the experiments. It can be observed

Table 1. Calculated parameters of model for methane under different conditions.

T_{exp} (K)	$P_{initial}$ (Bar)	A_r (J/mol)	t_K (sec)
274	45.13	-3982	2353
274	54.89	-3894	2392
274	69.16	-3900	2254
276	45.20	-5023	2341
276	55.11	-4051	2231
276	69.89	-6331	1274
276	79.25	-5753	1363
276	87.40	-4700	1827
278	56.35	-4049	2949
278	71.63	-4556	2818
278	78.71	-3074	3197
280	71.63	-3951	4068
280	81.36	-3963	3585
280	88.84	-4163	3414
282	82.68	-4157	4763
282	90.68	-4118	3711

Table 2. Calculated parameters of model for propane under different conditions.

T_{exp} (K)	$P_{initial}$ (Bar)	A_r (J/mol)	t_K (sec)
274	2.84	-9700	10267
274	3.38	-9543	6936
274	4.00	-9989	5061
274	4.28	-10000	6410
275	3.39	-10732	12977
275	4.08	-11876	10325
275	4.28	-9048	9890
276	4.43	-9390	15800

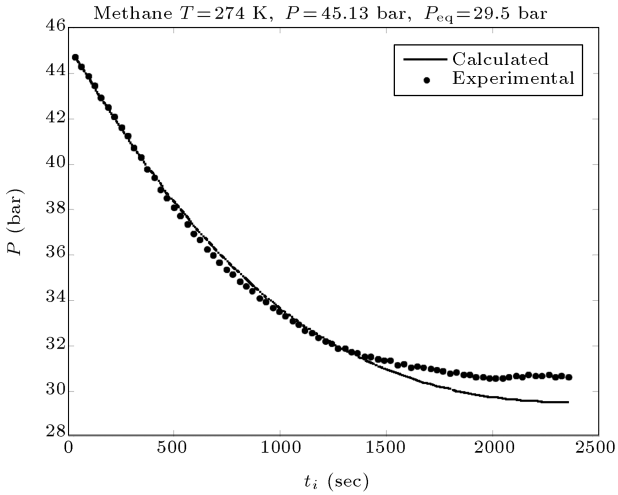

Figure 11a. Calculated and experimental rate data for methane ($T = 274$ K and $P_{initial} = 45.13$ Bar).

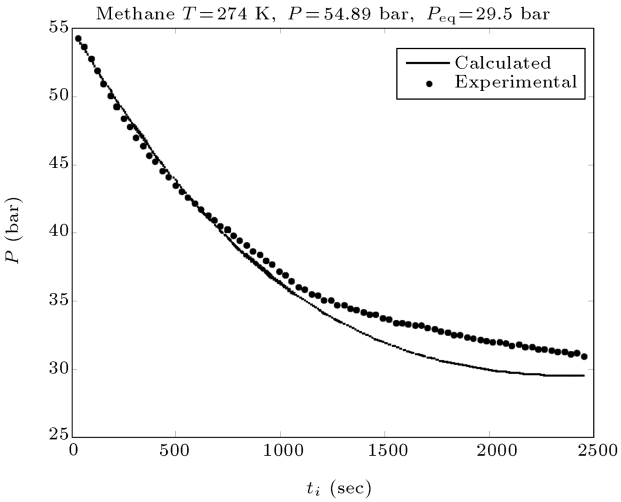

Figure 11b. Calculated and experimental rate data for methane ($T = 274$ K and $P_{initial} = 54.89$ Bar).

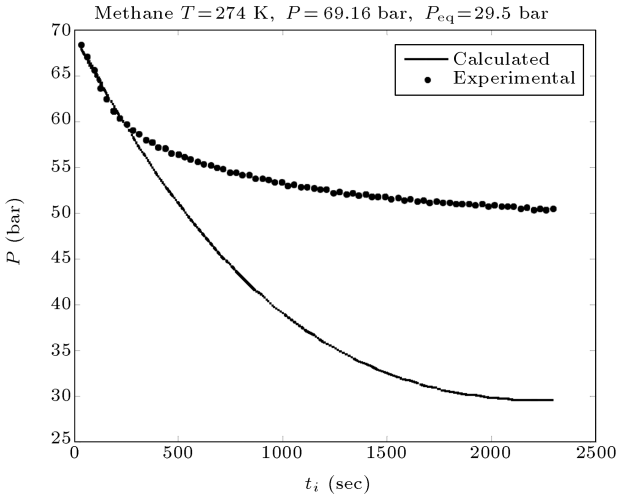

Figure 11c. Calculated and experimental rate data for methane ($T = 274$ K and $P_{initial} = 69.16$ Bar).

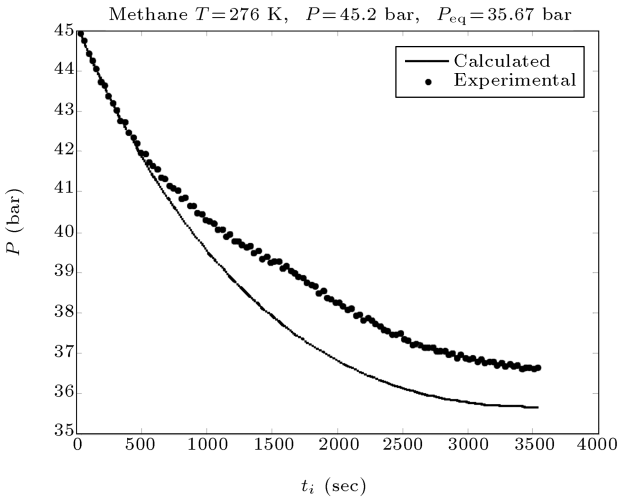

Figure 11d. Calculated and experimental rate data for methane ($T = 276$ K and $P_{\text{initial}} = 45.2$ Bar).

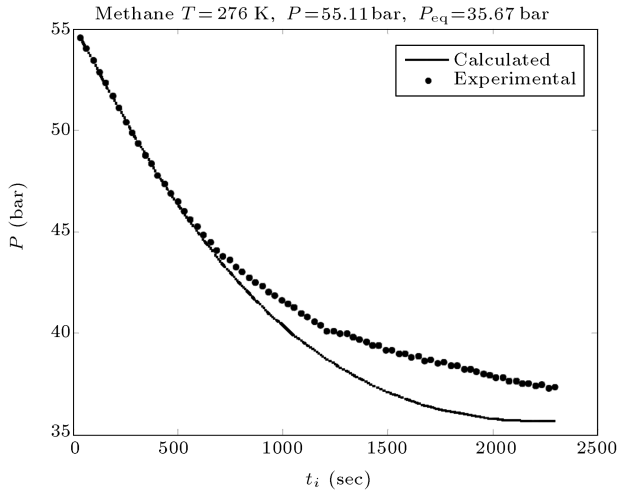

Figure 11e. Calculated and experimental rate data for methane ($T = 276$ K and $P_{\text{initial}} = 55.11$ Bar).

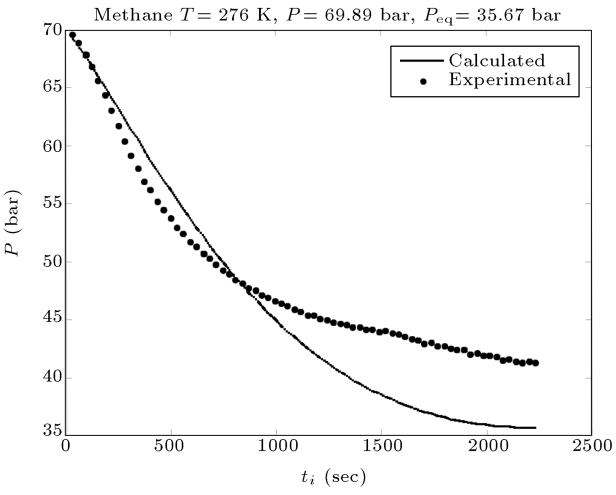

Figure 11f. Calculated and experimental rate data for methane ($T = 276$ K and $P_{\text{initial}} = 69.89$ Bar).

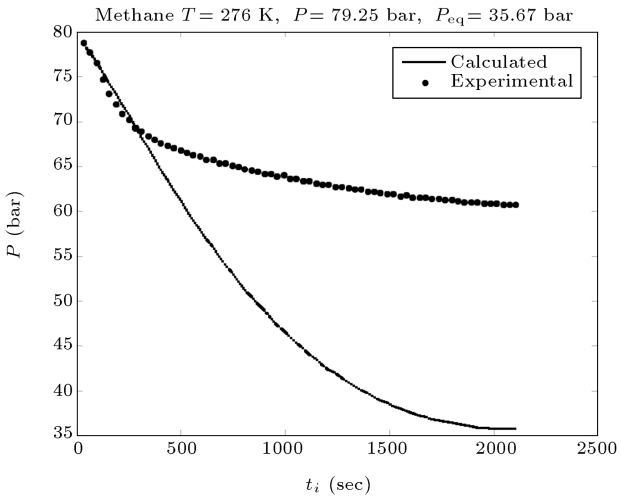

Figure 11g. Calculated and experimental rate data for methane ($T = 276$ K and $P_{\text{initial}} = 79.25$ Bar).

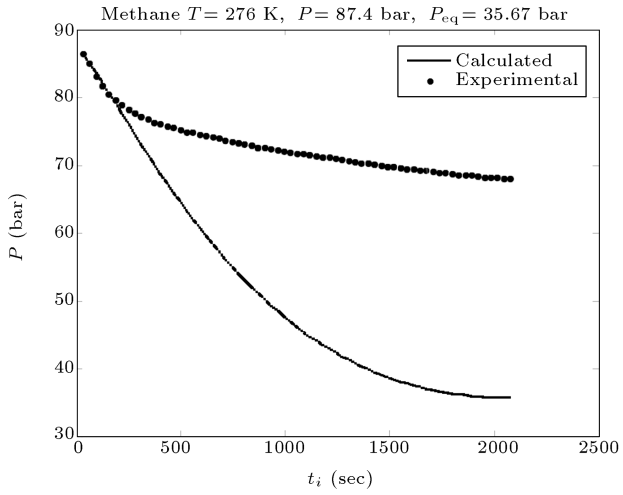

Figure 11h. Calculated and experimental rate data for methane ($T = 276$ K and $P_{\text{initial}} = 87.4$ Bar).

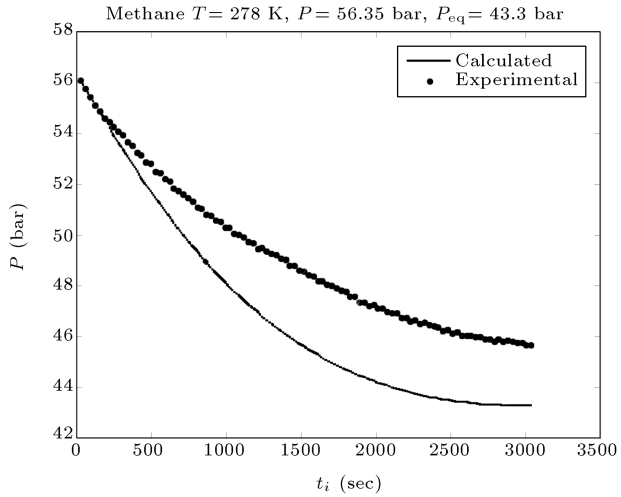

Figure 11i. Calculated and experimental rate data for methane ($T = 278$ K and $P_{\text{initial}} = 56.35$ Bar).

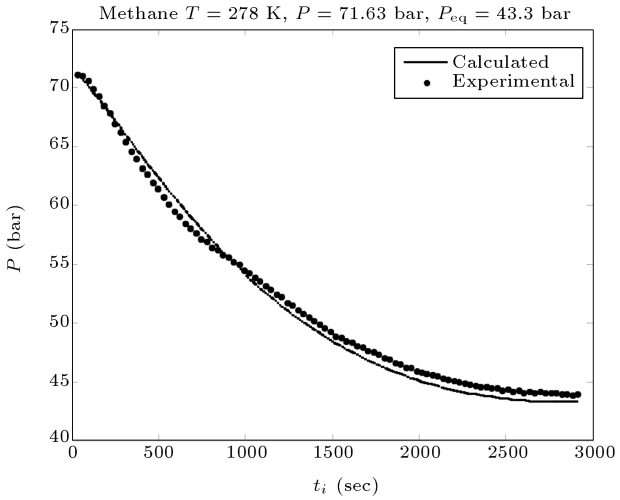

Figure 11j. Calculated and experimental rate data for methane ($T = 278$ K and $P_{\text{initial}} = 71.63$ Bar).

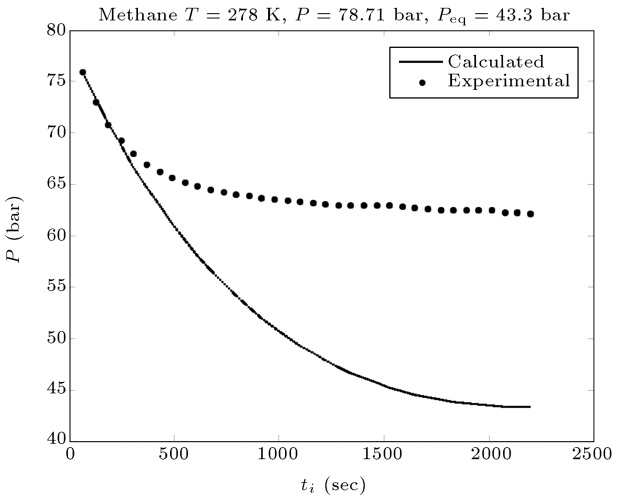

Figure 11k. Calculated and experimental rate data for methane ($T = 278$ K and $P_{\text{initial}} = 78.71$ Bar).

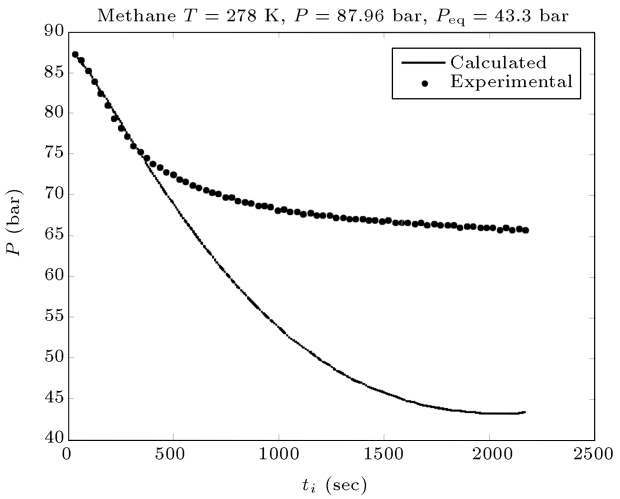

Figure 11l. Calculated and experimental rate data for methane ($T = 278$ K and $P_{\text{initial}} = 87.96$ Bar).

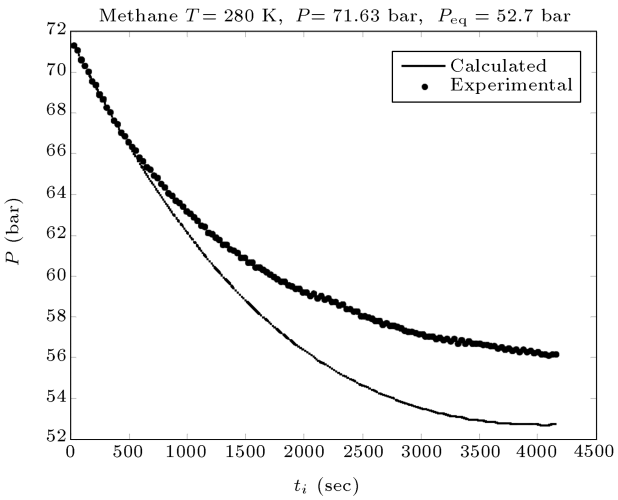

Figure 11m. Calculated and experimental rate data for methane ($T = 280$ K and $P_{\text{initial}} = 71.63$ Bar).

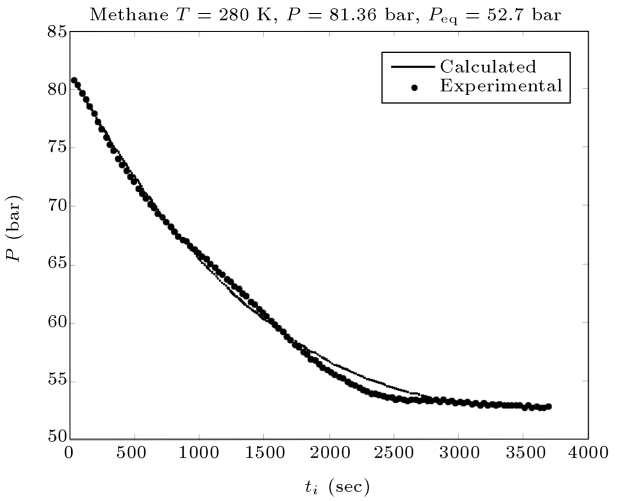

Figure 11n. Calculated and experimental rate data for methane ($T = 280$ K and $P_{\text{initial}} = 81.36$ Bar).

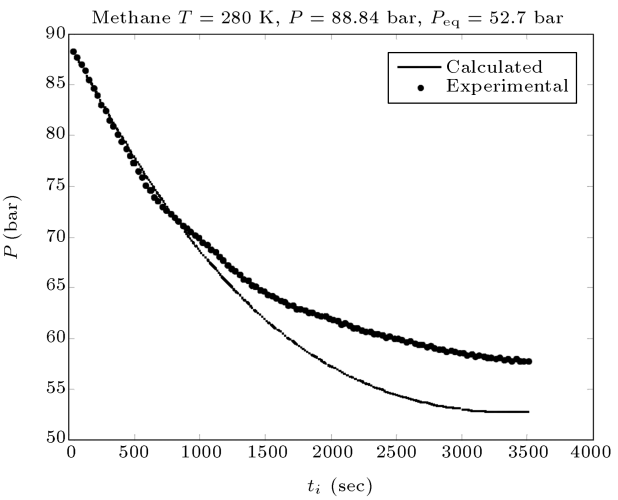

Figure 11o. Calculated and experimental rate data for methane ($T = 280$ K and $P_{\text{initial}} = 88.84$ Bar).

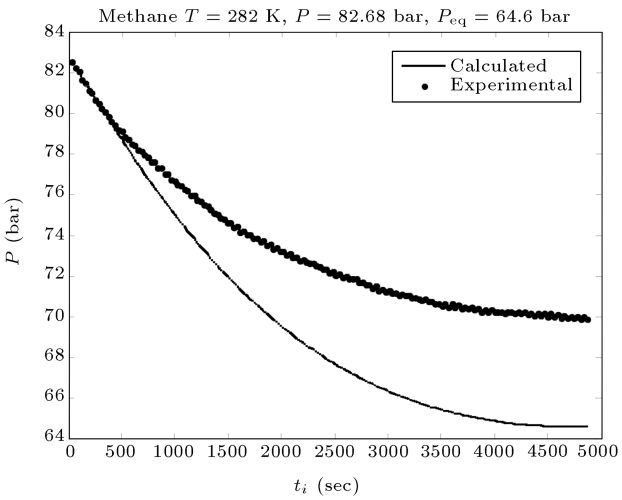

Figure 11p. Calculated and experimental rate data for methane ($T = 282$ K and $P_{\text{initial}} = 82.68$ Bar).

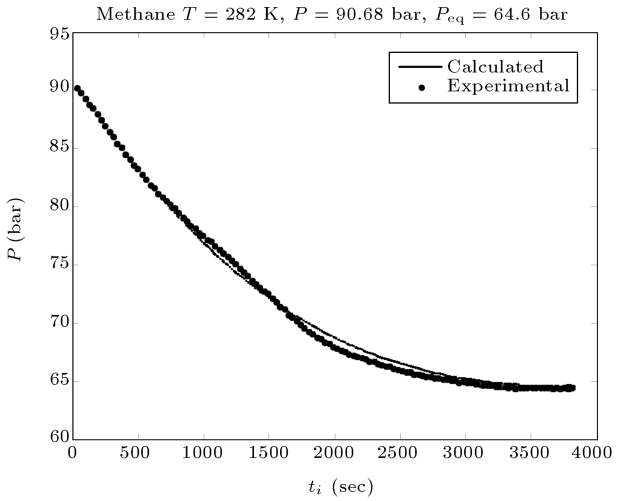

Figure 11q. Calculated and experimental rate data for methane ($T = 282$ K and $P_{\text{initial}} = 90.68$ Bar).

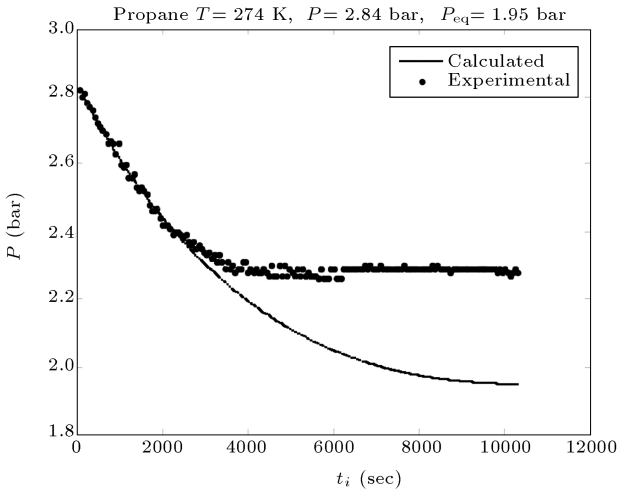

Figure 12a. Calculated and experimental rate data for propane ($T = 274$ K and $P_{\text{initial}} = 2.8$ Bar).

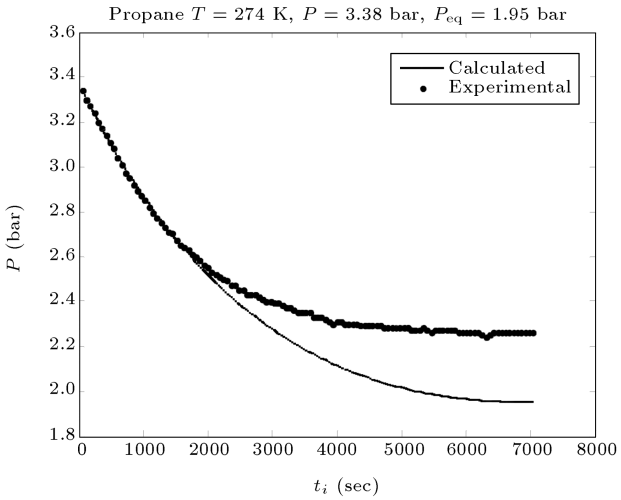

Figure 12b. Calculated and experimental rate data for propane ($T = 274$ K and $P_{\text{initial}} = 3.38$ Bar).

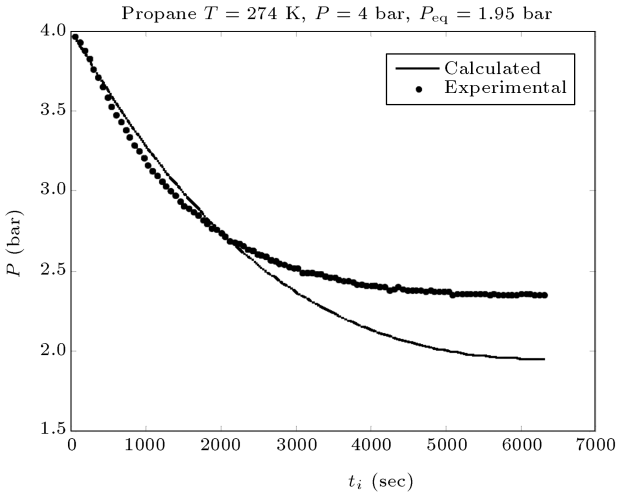

Figure 12c. Calculated and experimental rate data for propane ($T = 274$ K and $P_{\text{initial}} = 4.0$ Bar).

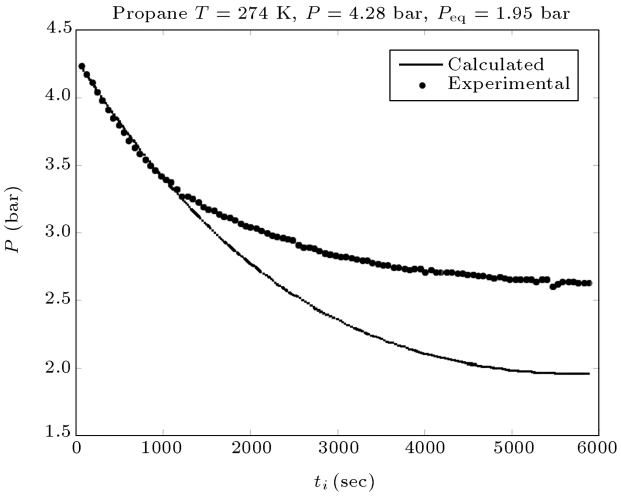

Figure 12d. Calculated and experimental rate data for propane ($T = 274$ K and $P_{\text{initial}} = 4.28$ Bar).

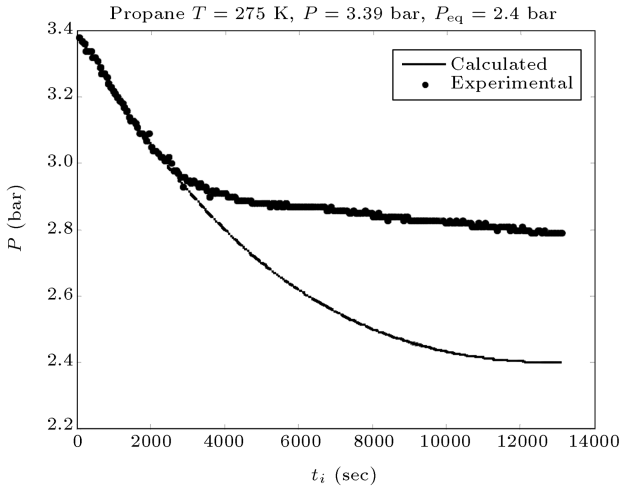

Figure 12e. Calculated and experimental rate data for propane ($T = 275$ K and $P_{\text{initial}} = 3.39$ Bar).

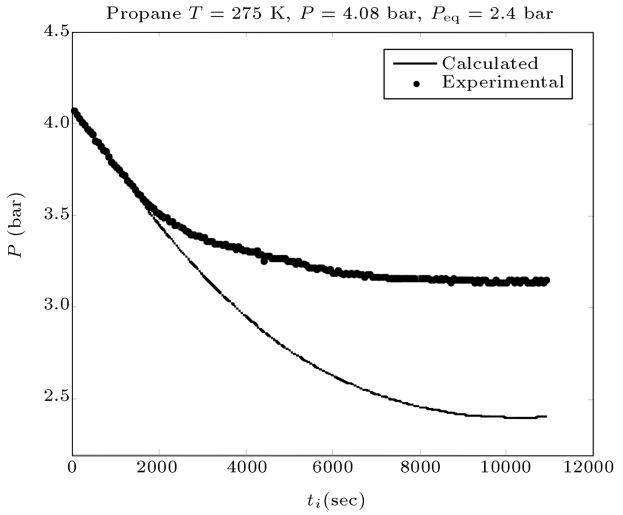

Figure 12f. Calculated and experimental rate data for propane ($T = 275$ K and $P_{\text{initial}} = 4.08$ Bar).

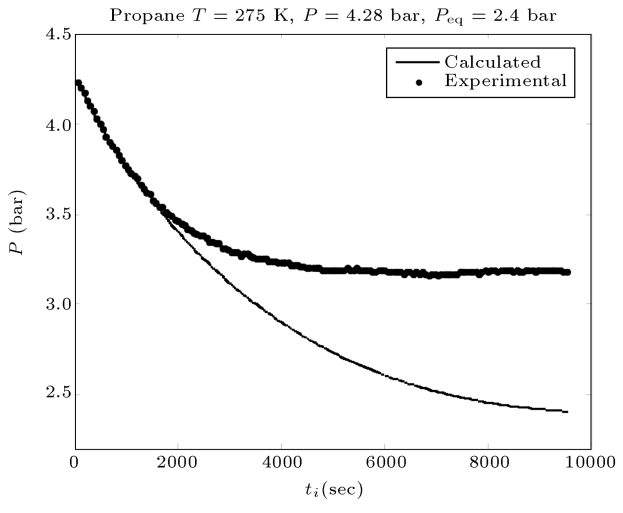

Figure 12g. Calculated and experimental rate data for propane ($T = 275$ K and $P_{\text{initial}} = 4.28$ Bar).

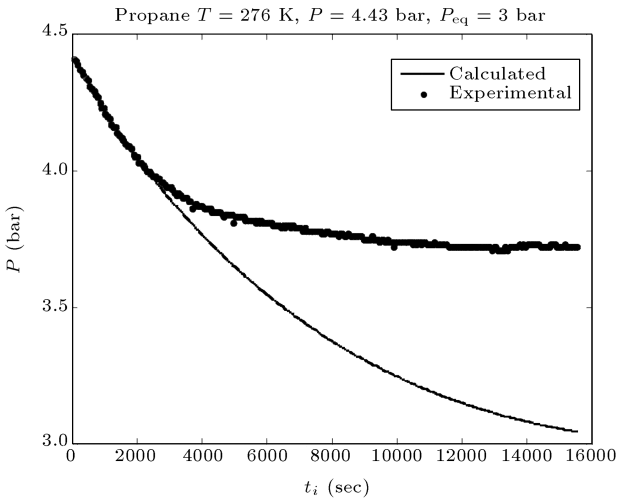

Figure 12h. Calculated and experimental rate data for propane ($T = 276$ K and $P_{\text{initial}} = 4.43$ Bar).

from high pressure experiments that the final pressure of the reactor is not P_{eq} (point B in Figure 2). Theoretically, the final pressure must be equal to the pressure of point B. We know that if the conditions of hydrate formation are far from equilibrium (high driving force or high initial pressure), the nuclei from crystallization will become very small and the rate of hydrate formation will be high; a large amount of hydrates would then form in a short time. If the mixing of the reactor were not sufficient (in our experiments, mixing is prepared by the movement of mercury in the reactor), hydrates would aggregate in the gas-liquid interfacial surface and reduce the mass transfer area; the kinetics of hydrate formation would be affected by the mass transfer of gas to liquid. These are the mainsprings of the differences between experimental and modeling results at high initial pressures; if there were good mixing within the reactor, the agreement of the model would be good. We ignored the last data of experiments that did not get the $P - \text{eq}$ in each experiment, and the calculation of A_r and t_k was based on first rate data. Also, this model can be applied for crystals I and II gases.

CONCLUSIONS

There are many models in literature for gas hydrate formation that use a microscopic driving force, like mass transfer from gas phase to water, or heat transfer between solid particles and the bulk of the liquid. Such models need experimental parameters, like mass transfer coefficients, heat transfer coefficients or population of particles, and these coefficients differ for each experiment. But, in this research, a conceptual model was proposed that defines a macroscopic driving force that only needs initial conditions (experimental condition, temperature and pressure) and final condi-

tions (equilibrium conditions). The basic idea is that there is a unique path for each experiment in which the crystallization process decays the affinity. Microscopic phenomena, such as mass transfer, heat transfer and nucleation, occur at their special rates and cause the overall formation rate, so that the time for this affinity decay is minimal. Because of the thermodynamic relation between affinity and Helmholtz free energy, this model can directly and easily be used for the gas mixture and predicting the A_r for pure gases.

NOMENCLATURE

a	chemical activity
A	chemical affinity
A_r	constant of proportionality
$\dot{A}_{T,V}$	affinity decay rate in constant temperature and volume
K	equilibrium constant
n	number of moles of gas that occupy the cavities
n_w	number of water molecules
NH	number of hydrate forming gases
N_{cav}	number of cavities in hydrate structure
P	pressure
Q	amount of equilibrium constant in non-equilibrium conditions
R	universal gas constant
t	time
t_k	time required to get equilibrium conditions
T	temperature
V	volume
Z	compressibility factor

Greek Letters

μ	chemical potential
ν	stoichiometric coefficient of reaction
ζ_Q	extent of reaction based on mole
ζ_{ti}	extent of reaction based on time

Subscripts

A	initial condition for hydrate formation
B	final condition for hydrate formation
i	arbitrary component
j	arbitrary data point

REFERENCES

1. Ma, O.L., Chen, G.J. and Guo, T.M. "Modeling the gas hydrate formation of inhibitor containing systems", *Fluid Phase Equilibria*, **205**, pp. 291-302 (2003).
2. Jager, M.D., Ballard, A.L. and Sloan, E.D. Jr. "The next generation of hydrate prediction. II. Dedicated aqueous phase fugacity model for hydrate prediction", *Fluid Phase Equilibria*, **211**, pp. 85-107 (2003).
3. Visniauskaas, A. and Bishnoi, P.R. "A kinetic study of methane hydrate formation", *Chem. Eng. Sci.*, **38**, pp. 1061-1072 (1983).
4. Visniauskaas, A. and Bishnoi, P.R. "Kinetics of ethane hydrate formation", *Chem. Eng. Sci.*, **40**, pp. 299-303 (1985).
5. Englezos, P., Kalogerakis, N., Dholabhai, P.D. and Bishnoi, P.R. "Kinetics of formation of methane and ethane gas hydrates", *Chem. Eng. Sci.*, **42**, pp. 2647-2658 (1987).
6. Varaminian, F. "The role of heat transfer in kinetics of hydrate formation", *Proceedings of the Fourth International Conference on Gas Hydrate*, Yokohama, pp. 465-468 (19-23 May 2002).
7. Clarke, M.A. and Bishnoi, P.R. "Determination of the intrinsic kinetics of CO_2 gas hydrate formation using in situ particle size analysis", *Chem. Eng. Sci.*, **60**, pp. 695-709 (2005).
8. Prigogine, I. and DeFay, R., *Chemical Thermodynamics*, Wiley, New York, USA (1962).
9. Garfinkle, M. "The thermodynamic natural path in chemical reaction kinetics", *Discrete Dynamics in Nature and Society*, **4**, pp. 145-164 (2000).
10. Garfinkle, M. "Non-equilibrium thermodynamics of closed-system reactions", *Materials Chemistry*, **7**, pp. 359-394 (1982).
11. Anklam, M.R. and Firoozabadi, A. "Driving force and composition for multi component gas hydrate nucleation from supersaturated aqueous solutions", *Journal of Chemical Physics*, **121**(23), pp. 11867-11874 (2004).

BIOGRAPHIES

Farshad Varaminian is an Associate Professor of Chemical Engineering at Semnan University in Iran. He received a B.S. degree from Isfahan University of Technology, and M.S. and Ph.D. degrees in Chemical Engineering from Tehran University, Iran. His current research interests are Kinetics of Formation and Decomposition of Gas Hydrates.

Amir Abbas Izadpanah is an Assistant Professor of Chemical Engineering at the Persian Gulf University in Bushehr, Iran. He holds a B.S. degree from Shiraz University, Iran, and M.S. and Ph.D. degrees in Chemical Engineering from Tarbiat Modaress University in Tehran, Iran. His current research interests include: Thermodynamics and Kinetics of Gas Hydrates, Equations of State and their Mixing Rule and Phase Envelope of Hydrocarbon Reservoirs.